JOURNAL OF OPTOELECTRONICS AND ADVANCED MATERIALS Vol. 27, Iss. 9 - 10, September - October 2025, p. 446 - 456

Design of quad HG modal full-duplex MDM-RoF system employing integrated SMF-FSO link under severe weather conditions

MEET KUMARI*
Department of ECE, UIE and UCRD, Chandigarh University, Mohali-140413, Punjab, India

In today world, mode division multiplexing (MDM) technology is essential to expand the data capacity of traditional radio-over-fiber (RoF) systems to accommodate massive cloud computing, big data, Internet of Things (IoT) and other broadband applications. In this work, a symmetric 1Gbps MDM based full-duplex RoF system using integrated single mode fiber and free space optics (SMF-FSO) channel is designed. Four Hermite Gaussian (HG) modes are transmitted over fixed 10km SMF with FSO range of 30-100m in downlink and 10-17m in uplink under air, haze, fog and rain scenarios. At 10m FSO range under same conditions, maximum beam divergence of 3.5-10mrad and additional loss of 0.3-5dB can be sustained, at error rate of 10^{-9}. Moreover, compared to prior works, this work provides optimum performance and can be used for high-capacity long-reach wired-wireless based systems.

(Received December 25, 2024; accepted October 14, 2025)

Keywords: FSO, HG, MDM, RoF

1. Introduction

In the past few years, the bandwidth demand of access networks for providing the high throughput data, like video services, is rising rapidly with considerable convenient access [1]. Radio-over-fiber (RoF) is an analogue communication system which directly distributes the radio frequency (RF) signals. RoF had led to the requirement for high-capacity optical communication systems that incorporate optical formations with high spectral efficiency [2]. This technology employs various benefits over the wireless and coaxial cable like low attenuation loss owing to fiber cable and large bandwidth (~THz) than the wireless frequency. However, its installation needs enough cost, but its maintenance cost is less and reduces the power consumption than wireless systems. It also provides operational flexibility and enhanced cellular coverage [3]. In [2], a sub-carrier multiplexing (SCM) and wavelength division multiplexing (WDM) based RoF incorporated passive optical network (PON) is realized over 80km single mode fiber (SMF) at 10Gbps data rate. In [4], a RoF-WDM-PON system over 20km SMF at 40Gbps is realized. In [5], a 5Gbps RoF system over 42km SMF and a 0.4m wireless link is presented.

Further, the integrated RoF and free space optics (FSO) has been seen as a complementing infrastructure where fiber deployment is not reachable. RoF/FSO system provides ultra-high speeds, license-free bandwidth utilization, network security and low power consumption over wireless networks at low cost [6]. Moreover, the capacity of recent fiber communication systems using has reached its limits, the feasibility of mode division multiplexing (MDM) has appeared to solve the Shannon limit capacity crunch [7].

Recently, in [8], a MDM based RoF i.e. MDM-RoF system using linearly polarized linearly polarized (LP[0,1]) mode over 2km fiber at 6Gbps data rate is demonstrated. Multiple-input multiple-output algorithm is capable of reconstructing the data signals by conquering distortion as well as crosstalk in fiber and radio frequency free-space channels. However, certain high-frequency roll-off is seen for the high-order modes owing to cross-coupling effects in the optical-fibre presenting modal dispersion. In another work, a MDM-RoF system over 15km fiber with 500m FSO range at 20Gbps data rate using Laguerre-Gaussian (LG) modes under different weather conditions is presented [9]. This system incorporates integration WDM and MDM by using LG[0,1] and LG[0,3] modes under clear air, mild haze, light rain, light dust, thin and thick fog with strong turbulence. But it again undergoes limited channel capacity. In [10], a 10Gbps RoF-FSO system using orthogonal frequency division multiplexing (OFDM) multiplexing over 15km fiber with 135m wireless range under non-uniform turbulence. It achieves minimum receiver sensitivity of -23dBm with transceiver gain of 25dBi, for 25GHz millimeter wave (mmW) communication. However, it possesses limited channel capacity, transmission range and data rate. In [11], a 8Gbps MDM system using quadrature phase shift keying (QPSK) modulation over 40cm THz link is demonstrated. Different LG modes are incorporated considering power and crosstalk losses. But the system performance decays as higher-order LG modes also increase beam divergence, beam size as well as power loss. Moreover, in [12], a 120Gbbps OFDM-FSO system using LG beams over 400m range under light and heavy dust with strong turbulence scenario is proposed. The system offers high SNR with beam divergence of 0.2mrad. But the presence of high input power of 20dBm for multiple LG beams can limit the signal capacity as well it also suffers from limited transmission range. An orthogonal chirp division multiplexing with orbital angular momentum (OCDM-OAM) system using OFDM multiplexing at 6.82Gbps data rate is realized successfully [13]. This mechanism provides the high-security in the system but also suffers from higher system complexity and cost. In [14], a passive optical network (PON) wireless integrated access network is demonstrated. It offers OFDM signals transmission over optical wireless communication as well a visible light communication at 15Gbps data rate over short-range of 10m. Thus, inspired from earlier works, it is realized that the due to impact of severe weather conditions, the RoF based systems are still lacking in transmission range, throughput and channel capacity.

Recent trends of rapidly growing retirement for high-capacity as well as high-speed access network lead optical access networking research for coherent network [10–14]. To take full benefit of THz band- width which can be shared among numerous subscribes with a narrow bandwidth is a difficult task without incorporating coherent scheme. High-capacity optical networks can draw advantages from simple architecture together with MDM multiplexing, via improving spectral efficiency and lessening the bandwidth requirement optoelectronic components. Meanwhile, MDM based RoF technology is considered to be an effective decision to provide gigabit wireless access [15].

Motivation of this work is to realize a cost effective and simple design of bidirectional RoF-MDM system using an integrated SMF-FSO link under the impact of different atmospheric conditions and link losses. The system's reliability is investigated considering diverse performance metrics like eye patterns, optical spectra, bit error rate (BER) and timing diagrams with maximum 10km SMF and 100m FSO distance at BER limit of 10^{-9}. To validate, the obtained results are compared with recent articles (last 3-5 years) in terms of different parameters.

The major contributions of this paper are:

- Design and investigate a 1Gbps quad Hermite Gaussian (HG) modal full-duplex MDM-RoF system using SMF-FSO under different weather conditions
- Investigate the system performance for varied FSO range, divergence and additional loss for various HG modes under clear air.
- Comparative analysis w.r.t. existing designs based on different parameters.

Here, Section 2 illustrates the proposed design of MDM-RoF system. The results analysis are depicted in Section 3 followed by the conclusion in Section 4.

2. Proposed design

Fig. 1 depicts the proposed design of a MDM-RoF system using HG[0,0], HG[1,0], HG[2,0] and HG[3,0] modes. As compared to LG modes, HG modes offer simpler coupling to detectors and fibers, better localization and better cartesian symmetry for positioning system.

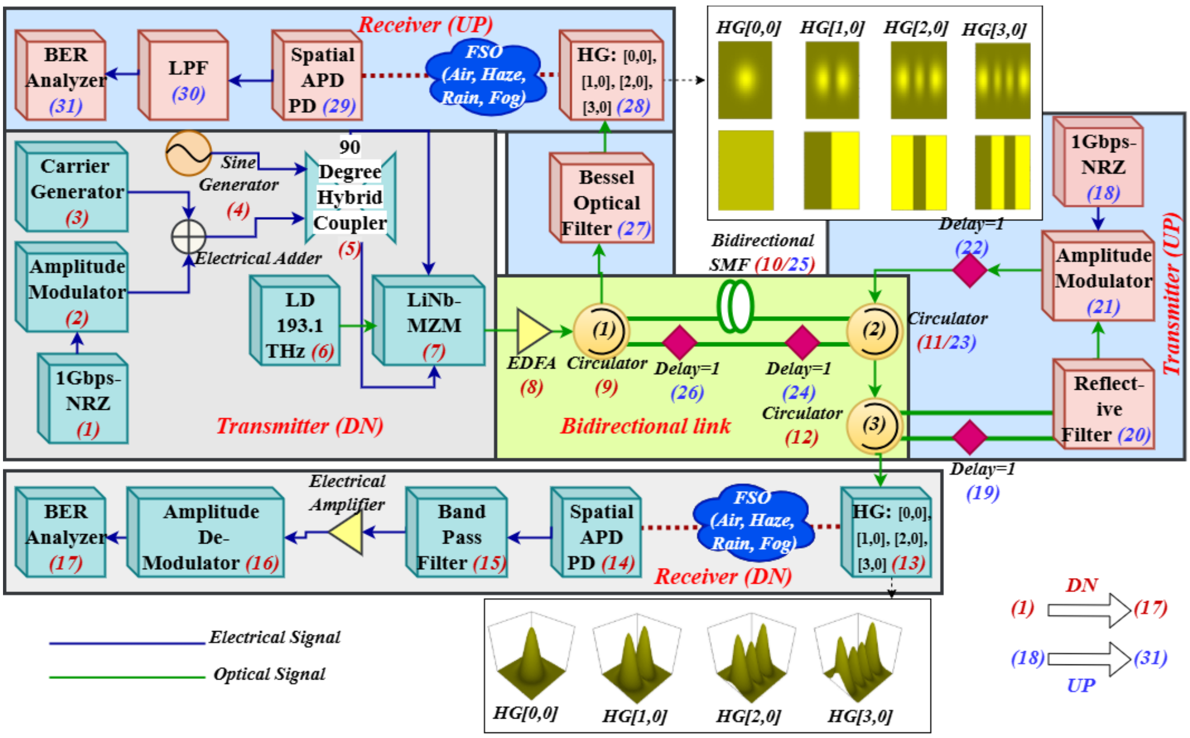

Fig. 1. Proposed quad HG modal MDM-RoF system incorporating integrated SMF-FSO link, insets: generated modes (colour online)

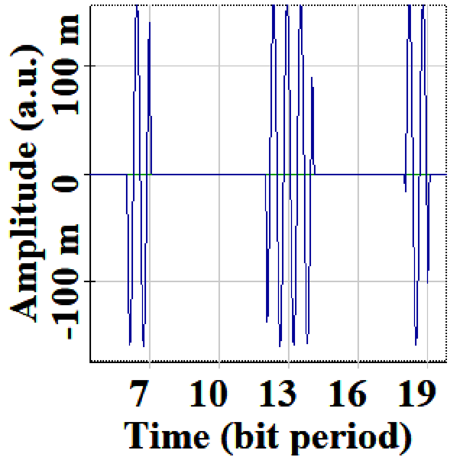

Timing diagram at Tx

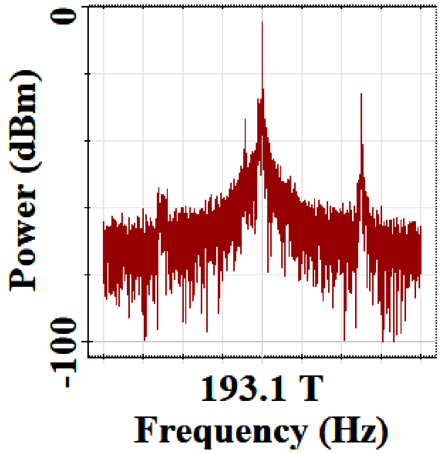

Optical spctrum at Tx

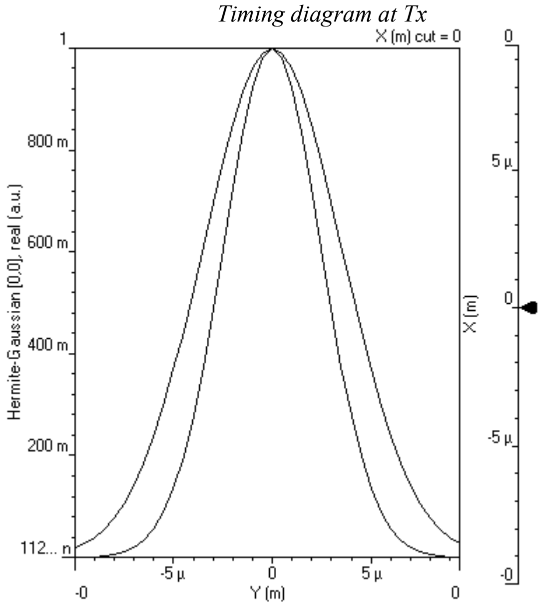

2D-view HG[0,0]

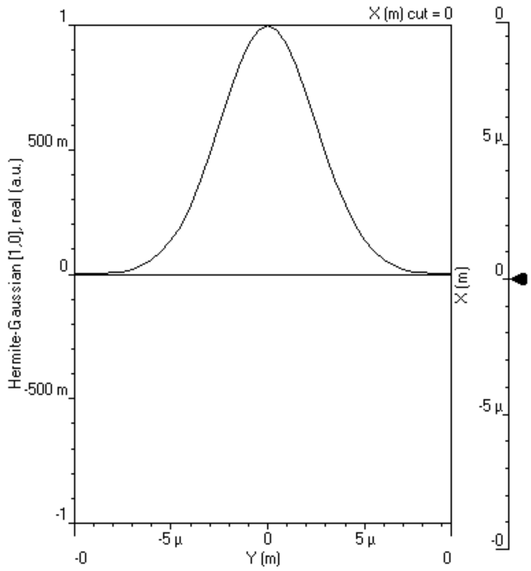

2D-view HG[1,0]

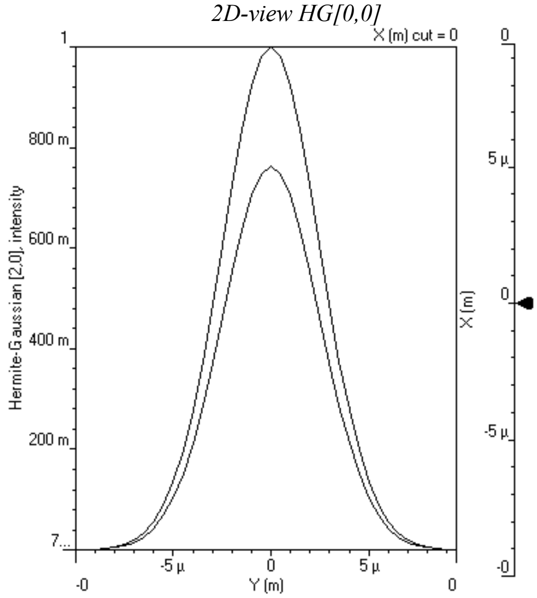

2D-view HG[2,0]

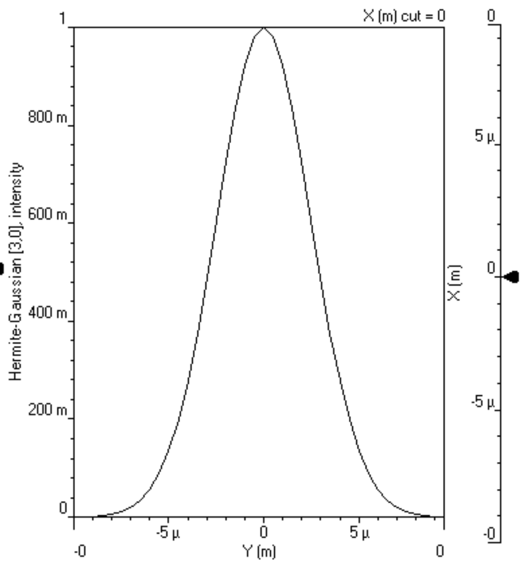

2D-view HG[2,0]

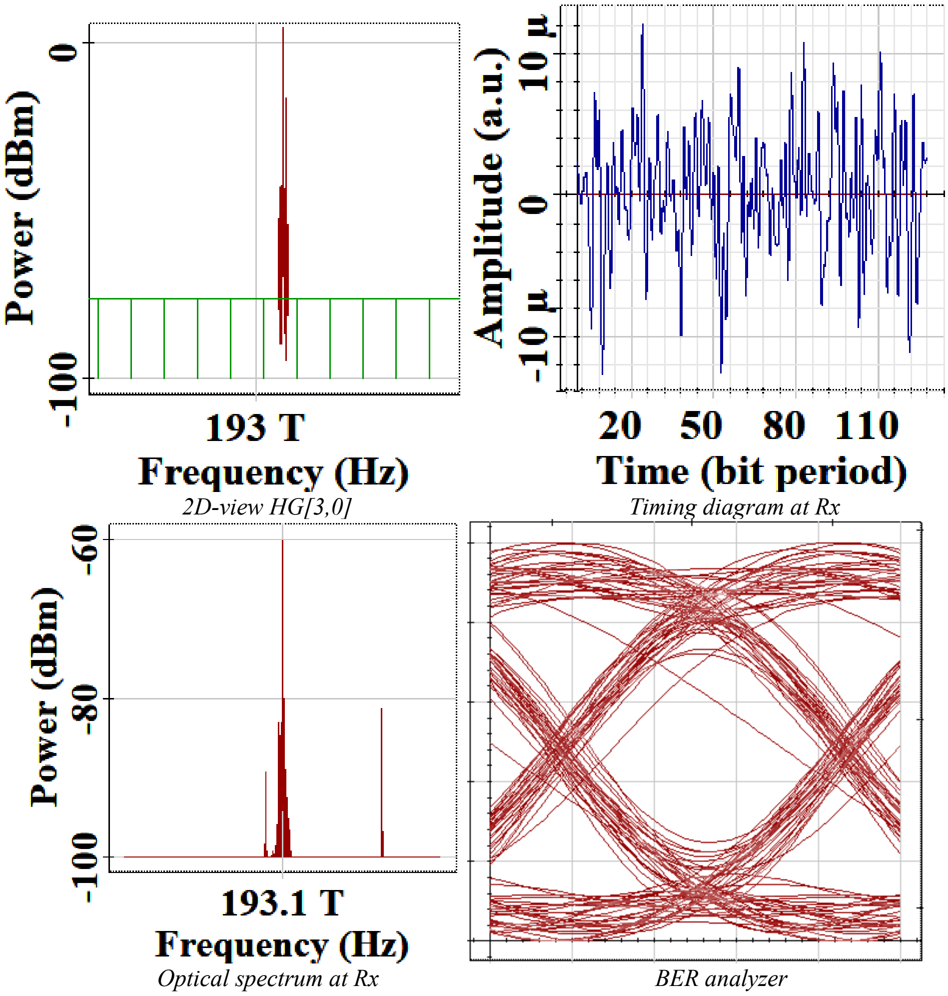

Fig. 2. Spectra and eye pattern realized in the proposed system (colour online)

Proposed RoF-MDM system is designed and investigated in OptiSystem v. 20 simulation tools. OptiSystem is an innovative, powerful & rapidly advancing software tool, enabling users for planning, testing & simulating many types of optical networks. It allows short-to-long distance data transmission at high speed in different optoelectronic systems. It also offers optical systems design (transmission layer) and visually represents system performances analysis.

In downlink (DN) transmission, the light signal at the 193.1THz wavelength with 10MHz linewidth, is firstly generated via a continuous wave laser diode (LD). This signal is utilized for external modulation of a LD via a LiNb Mach-Zehnder modulator (MZM) having 30dB extinction ratio and 4V bias voltage. MZM is used to modulate the intensity, frequency and phase of light. Its operations are based on the interference principle. After this, to realize the SCM amplitude shift keying (ASK) signal to MZM, the amplitude modulator is used. SCM-ASK is a scheme where multiple radio RF subcarriers are modulated utilizing ASK and then multiplexed to be modulated with an optical carrier. Then, the modulation signal is added with an optical carrier generator via an electrical adder. The data is transmitted at 1Gbps in non-return to zero data format. In downlink, a 90 deg hybrid coupler i.e. a four-port passive RF device, which split an incoming signal into two outputs (in equal amplitude and 90 deg phase difference), is employed. The resultant signal obtained from a 90deg hybrid coupler with inputs from a sine generator (frequency=10GHz) as well as electrical adder output is forwarded to MZM. Then, the modulated signal is passed through an Erbium doped fiber amplifier (power=10dBm, noise figure=5dB) for signal amplification followed by three bidirectional circulators (circulator 1 to 2 and then 3) to realize the bidirectional transmissions. The optical delays devices (=1 unit) are used for differentiating DN and uplink (UP) transmissions in the bidirectional SMF links. Fig. 2 depicts obtained spectra and eye pattern realized in OptiSystem tool. Fig. 3 presents the bidirectional transmission of the proposed system which incorporates three circulators to transmit the both downlink and uplink data simultaneously.

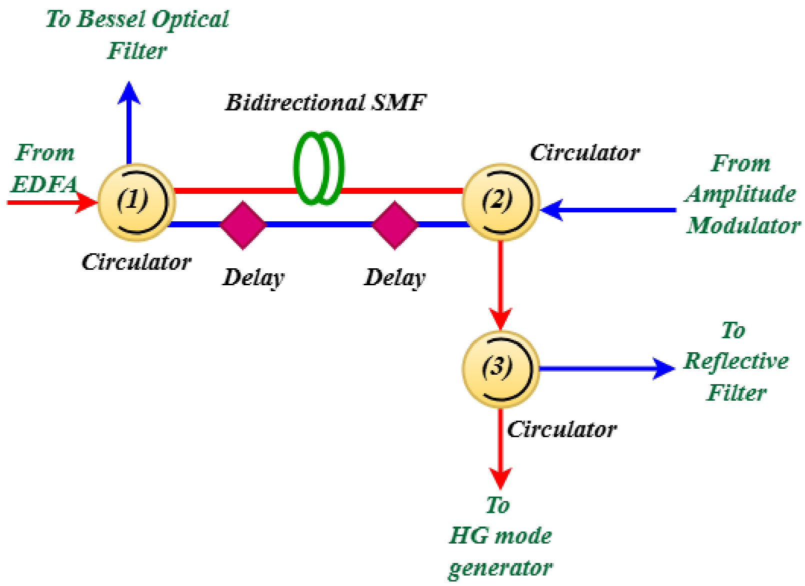

Fig. 3. Concept of bidirectional transmission in the proposed system (colour online)

For UP transmission, the received DN signal is passed through a reflective filter which reflects same frequency as for DN (193.1THz). It is followed by an amplitude modulator operating at symmetric data rate of 1Gbps over a bidirectional SMF by using delay units. After passing the signal from specified circulators (circulator 2 to 1), the signal is passed to receiver section. In both DN and UP receiver sections, a FSO channel is used under the impact of different atmospheric conditions. Also, a mode generator is used to generate different HG modes, in both DN and UP transmissions. A spatial avalanche photodiode is used to obtain the electrical equivalent signal of light signal. Additionally, an amplitude demodulator (gain=1) is utilized in DN reception followed by a filter (low pass) passing all required signals (lower frequency) for evaluating system BER performance. A Bessel optical filter offers linear phase, preserve pulse shape, minimize signal distortion and maintains constant group delay through the passband. A band-pass filter is used for signal selection as well as noise reduction. Insets show the generated HG modes' intensity and phase profiles. Table 1 depicts the simulation specifications used in the system design. HG mode at operating wavelength, λ is defined as [16]:

$$\Psi_{s,t}(q\emptyset) = H_s\left(\frac{\sqrt{2m}}{W_0^2 m}\right) exp\left(-\frac{m^2}{W_0^2 m}\right) exp\left(j\frac{\pi m^2}{\lambda r_0 m}\right) H_t\left(\frac{\sqrt{2m}}{w_0 n}\right) exp\left(-\frac{n^2}{W_0^2 n}\right) exp\left(j\frac{\pi n^2}{\lambda r_0 n}\right) \quad (1)$$

where s and t mean the X and Y index defining mode dependencies at X- and Y-axis, r_0 and W_0 exhibit radius of curvature and spot size respectively.

Table 1. Simulation specifications [17]

Parameter	Value
Launch power (dBm)	6
Linewidth (MHz)	10
Sine generator frequency (GHz)	10
Frequency (THz)	193.1
SMF range (km)	10
Fiber attenuation (dB/km)	0.2
Dark current (nA)	10
FSO range (m)	10-100
Throughput (Gbps)	1
Temperature (K)	300
Dispersion (ps/nm/km)	16.75
FSO Attenuation (dB/km)	0.2 (clear air), 4.2 (haze), 9.2 (rain), 20 (fog)
Geometric loss	Yes
Scintillation model	Gamma-Gamma
Index refraction structure ($m^{-2/3}$)	10^{-17}
Additional loss (dB)	0-5
Aperture diameter (cm)	20
Beam divergence (mrad)	0.5-5
Thermal noise (W/Hz)	10^{-22}
Shot noise	Yes
Responsivity (A/W)	1
BPF bandwidth (GHz)	1
Circulator return loss (dB)	60
Insertion loss (dB)	2

3. Results analysis

3.1. Integrated SMF-FSO channel model

The system performance is analyzed in OptiSystem v.22 at different HG modes over fixed 10-100m FSO range and fixed 10km SMF range at data rate of 1Gbps. Here, different atmospheric weather conditions are considered viz. air, fog, haze & rain (22.5mm/hr) in Gamma-Gamma distribution and it is described as:

$$J_{h_a}(h_a) = \frac{2(uv)^{\left(\frac{u+v}{2}\right)}}{\Gamma(u)\Gamma(v)} . h_a^{\left(\frac{u+v}{2}\right)-1} K_{u-u}\left[2(uvh_a)^{\frac{1}{2}}\right] \quad (2)$$

where $\Gamma(.)$ is Gamma function, K_{u-v} neams Bessel function of order $(u-v)$, u depicts irradiance fluctuations at large-scale, v = irradiance fluctuations at small scale. The value of both u and v are defined as:

$$u = \frac{1}{\left[exp\left\{\frac{0.49g_0^2}{\left(1+0.18e^2+0.56g_0^{\frac{12}{5}}\right)^{\frac{7}{6}}}\right\}-1\right]} \quad (3)$$

and

$$y = \frac{1}{\left[exp\left\{\frac{0.51g_0^2\left(1+0.18e^2+0.56g_0^{\frac{12}{5}}\right)^{\frac{-5}{6}}}{\left(1+0.90e^2+0.62e^2g_0^{\frac{12}{5}}\right)^{\frac{5}{6}}}\right\}-1\right]} \quad (4)$$

where g_0^2 is Rytov variance, e is spherical wave diameter. The system BER is given as [18]:

$$BER = \frac{1}{2} erfc\sqrt{\frac{Signal\ to\ Noise\ Ratio}{8}} \quad (5)$$

Again, the received power under diverse weather conditions is given as:

$$P_r = P_t . \left(\frac{A_r}{(\emptyset L)^2}\right) . exp(-\alpha L) \quad (6)$$

where P_r, P_t, A_r, $\emptyset$, L and α indicate transmitted power, received power, effective Rx aperture area, beam divergence, FSO range and attenuation coefficient respectively. Rain attenuation coefficient α_{rain} at rain rate, E is expressed as [18]:

$$\alpha_{rain} = \beta E^T \quad (7)$$

where β and T are coefficients depending on temperature and wavelength, λ. Also, haze attenuation coefficient, α_{haze} in Beer-Lambert Law is given as [18]:

$$\alpha_{haze} = e^{-\partial L} \quad (8)$$

where ∂ means haze attenuation coefficient. Moreover, snow attenuation coefficient, α_{fog} with visibility range, V is represented as [19]:

$$\alpha_{fog} = \frac{\frac{3.91}{V}\left(\frac{\lambda}{550}\right)^{-T}}{0.22} \quad (9)$$

3.2. Impact of various HG modes on FSO range under different weather conditions

Fig. 4(a)-4(h) depicts the BER performance of the system for different HG modes under distinct weather conditions in downlink and uplink direction.

Note that, HG[0,0] mode offers best performance over HG[1,0] followed by HG[2,0] and HG[3,0] for all weather conditions over fixed 10km SMF distance. Also, the BER shows best performance under air condition followed by haze, rain & fog weather conditions. The atmospheric conditions can result in random phase-front distortions on the transmitted HG beam, resulting in scintillation as well as beam wandering which induces power loss of the received signal and low SNR. The impact of phase front distortions aims to become larger for shorter wavelengths, long-reach distances, and higher turbulence value, which is considerably wavelength independent when realizing THz frequencies. Also, the received signal could be attenuated owing to atmospheric absorption by water molecules which can degrade the SNR and thus system BER performance [20]. Mathematically, the received power under the impact of different atmospheric conditions is given in equation (6).

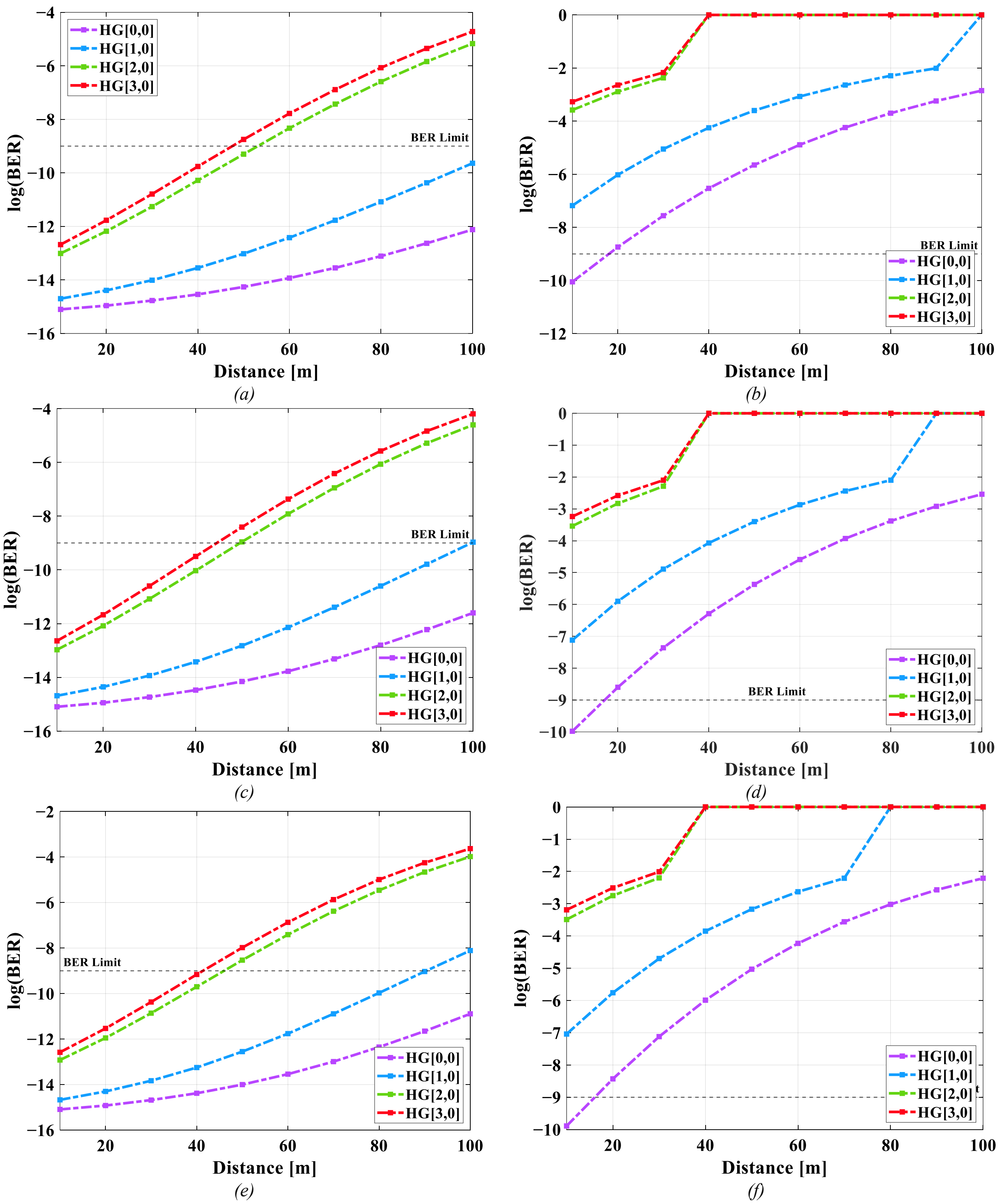

HG[0,0]
HG[1,0]
HG[2,0]
HG[3,0]
BER Limit
log(BER)
Distance [m]
(a)
(b)
(c)
(d)
(e)
(f)

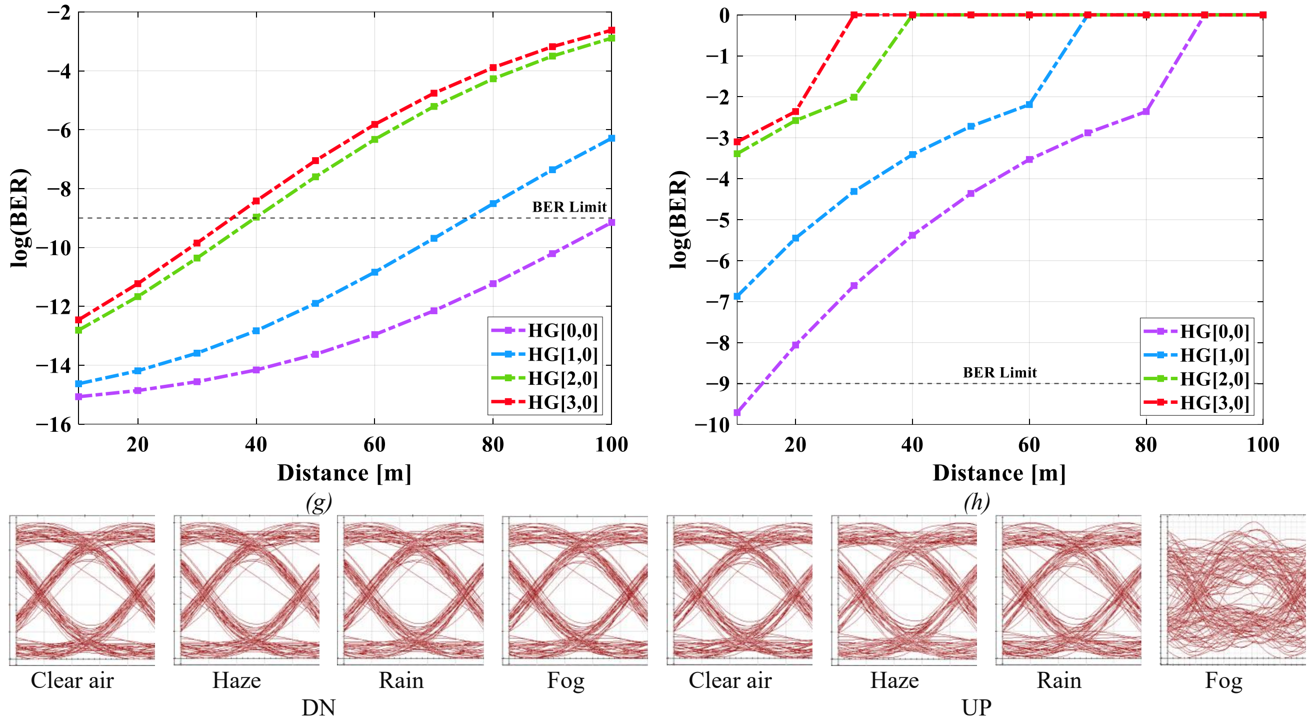

Fig.4. BER vs. FSO range for different HG modes under clear air weather in (a) DN, (b) UP; under haze weather in (c) DN, (d) UP; under rain weather in (e) DN, (f) UP; under fog weather in (g) DN and (h)UP directions; insets: corresponding eye patterns for HG[0,0] mode at 100m distance (colour online)

Fig. 4(a) exhibits faithful FSO range of 100, 100, 50 and 45m range for HG[0,0], HG[1,0], HG[2,0] and HG[3,0] modes respectively, in DN transmission under clear air. In uplink transmission, maximum FSO range of 17, <10, <10 and <10m for HG[0,0], HG[1,0], HG[2,0] and HG[3,0] modes respectively, under clear air weather, as shown in Fig. 4(b). Fig. 4(c) depicts faithful FSO range of 100, 100, 50 and 44m range for HG[0,0], HG[1,0], HG[2,0] and HG[3,0] modes respectively, under haze condition, in downlink transmission. Maximum FSO range of 16, <10, <10 and <10m for HG[0,0], HG[1,0], HG[2,0] and HG[3,0] modes respectively, under haze weather, in uplink transmission, as exhibited in Fig. 4(d). Fig. 4(e) depicts maximum FSO range of 100, 90, 45 and 40m range for HG[0,0], HG[1,0], HG[2,0] and HG[3,0] modes respectively, under rain condition, in downlink transmission. Maximum FSO range of 15, <10, <10 and <10m for HG[0,0], HG[1,0], HG[2,0] and HG[3,0] modes respectively, under rain weather, in uplink transmission, as exhibited in Fig. 4(f). Fig. 4(g) depicts maximum FSO range of 100, 75, 40 and 30m range for HG[0,0], HG[1,0], HG[2,0] and HG[3,0] modes respectively, under fog, in downlink transmission. Maximum FSO range of 14, <10, <10 and <10m for HG[0,0], HG[1,0], HG[2,0] and HG[3,0] modes respectively, under fog weather, in uplink transmission, as exhibited in Fig. 4(h).

Moreover, the clear wide opened eye patterns in DN than UP transmission exhibit the superiority of former for various modes and for different atmospheric conditions. Tables 2 and 3 depict the summarized results of faithful FSO range in the system for DN and UP transmission.

Table 2. Maximum FSO range (m) for various HG modes and weather conditions in DN

Weather	HG[0,0]	HG[1,0]	HG[2,0]	HG[3,0]
Clear air	100	100	50	45
Haze	100	100	50	44
Rain	100	90	45	40
Fog	100	75	40	30

Table 3. Maximum FSO range (m) for various HG modes and weather conditions in UP

Weather	HG[0,0]	HG[1,0]	HG[2,0]	HG[3,0]
Clear air	17	<10	<10	<10
Haze	16	<10	<10	<10
Rain	15	<10	<10	<10
Fog	14	<10	<10	<10

3.3. Impact of beam divergence on different modes

Fig. 5(a) and 5(b) present the BER performance of the system for distinct HG modes under clear air in downlink and uplink transmission respectively, for varied beam divergence.

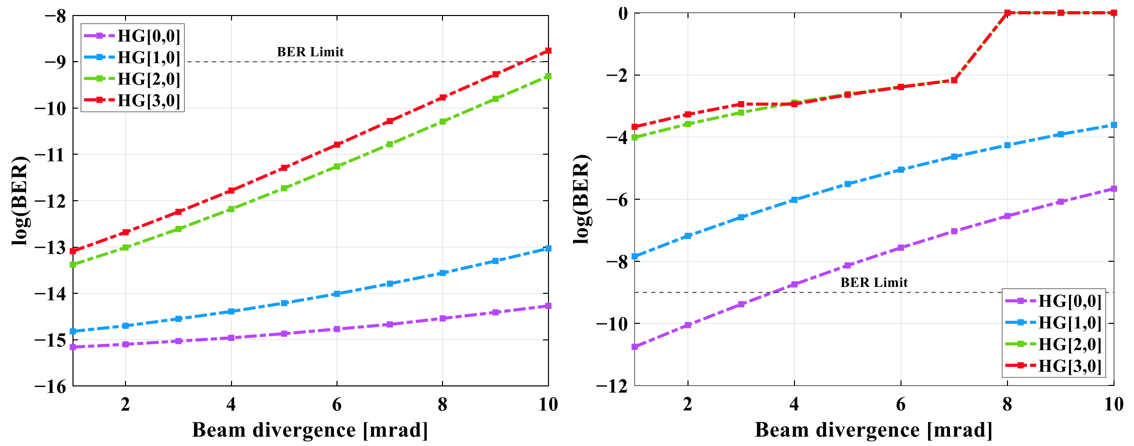

(a) *(b)*

Fig. 5. BER vs. beam divergence for different HG modes under clear air weather in (a) DN and (b) UP directions (colour online)

In FSO link, the beam divergence relies on several parameters, incorporating propagation distance, operating frequency, and mode order. In order to recover the transmitted beam, a larger receiver aperture could be required with enough signal power and reduce the BER [20]. The generated beam divergence in FSO transceiver section, results in the geometric loss and it is given as $GL(L) = \frac{A_r}{\pi}\left(\frac{2}{L\emptyset}\right)^2$ [21]. Again, HG[0,0] mode offers best performance over HG[1,0] followed by HG[2,0] and HG[3,0] over fixed 10km SMF and 10m FSO distance. It is due to maximum power dissipation in fundamental mode than higher modes. Further, the BER shows optimum performance at $\leq 10^{-9}$ under clear air condition in downlink than uplink direction. Fig. 5(a) shows that the system can sustain maximum beam divergence of >10, >10, >10 and 9.5mrad for HG[0,0], HG[1,0], HG[2,0] and HG[3,0] modes respectively, in downlink. Moreover, in uplink direction, maximum beam divergence of 3.5, <0.5, <0.5 and <0.5mrad is obtained for HG[0,0], HG[1,0], HG[2,0] and HG[3,0] modes respectively, as depicted in Fig. 5(b). Table 4 depict the summarized results of sustainable beam divergence in FSO link for both DN and UP transmissions.

Table 4. Maximum acceptable beam divergence (mrad) at 10e-9 BER in DN and UP transmission

TX	HG[0,0]	HG[1,0]	HG[2,0]	HG[3,0]
DN	>10	>10	>10	9.5
UP	3.5	<0.5	<0.5	<0.5

3.4. Impact of additional losses on different modes

Fig. 6(a) and 6(b) depict the BER performance of the system for distinct HG modes under clear air in downlink and uplink transmission respectively, for varied additional loss.

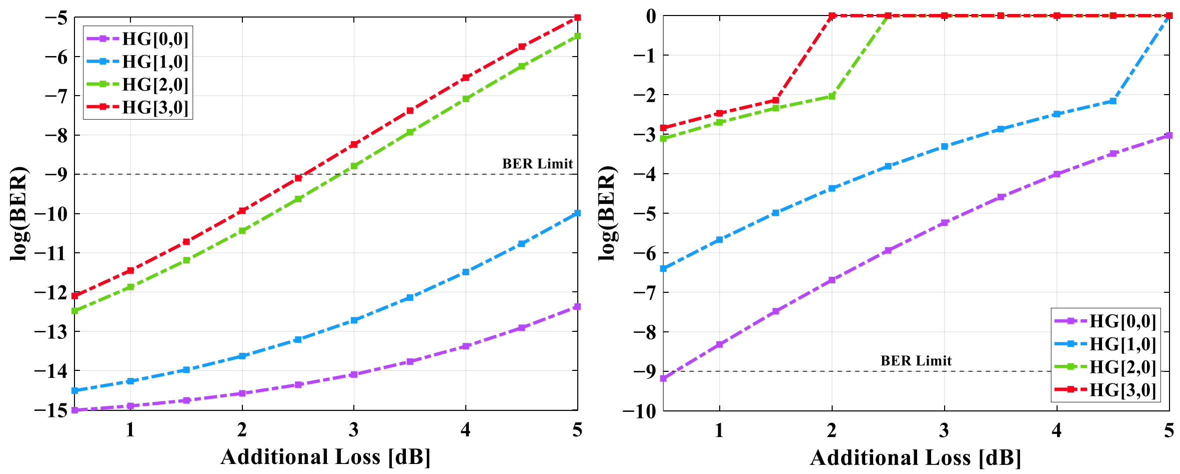

(a) *(b)*

Fig. 6. BER vs. additional loss for different HG modes under clear air weather in (a) DN and (b) UP directions; insets: corresponding eye patterns (colour online)

It is realized that HG[0,0] mode provides best performance over HG[1,0], HG[2,0] and HG[3,0] over fixed 10km SMF and 10m FSO distance. The BER limit of 10^{-9} under clear air condition is successfully obtained in downlink transmissions than uplink direction. Fig. 6(a) shows that the system incorporates maximum additional loss of >5, >5, 2.8 and 2.5dB for HG[0,0], HG[1,0], HG[2,0] and HG[3,0] modes respectively, in downlink direction. While in uplink direction, additional loss of 0.3, <0.1, <0.1 and <0.1dB is realized for BER limit of 10^{-9}, for HG[0,0], HG[1,0], HG[2,0] and HG[3,0] modes respectively, as depicted in Fig. 6(b). Table 5 depict the summarized results of sustainable beam divergence in FSO link for both DN and UP transmissions.

Table 5. Maximum acceptable additional loss (dB) at 10e-9 BER in DN and UP transmission

TX	**HG[0,0]**	**HG[1,0]**	**HG[2,0]**	**HG[3,0]**
DN	>5	>5	2.8	2.5
UP	0.3	<0.1	<0.1	<0.1

Table 6 depicts that the proposed system shows best performance as compared to existing designs.

Table 6. Comparison Analysis of exiting work and the proposed work

System characteristics		[10]	[9]	[11]	[12]	[13]	[22]	[23]	[24]	[14]	Proposed System
Year of publication		2020	2016	2022	2023	2024	2024	2024	2025	2025	
Max. Throughput		10Gbps	20Gbps	8Gbps	120Gbps	6.82Gbps	100Gbps	25Gbps	10Gbps	15Gbps	1Gbps
Modulation		OFDM	On-off keying (OOK)	QPSK	OFDM	OFDM	OFDM	OOK	OOK	OFDM	OOK
Input power		6dBm	10dBm	-	20dBm	15dBm	200mW	-	20dBm	12dBm	6dBm
Range	Wired	15km	15km	-	-	-	-	1km	10km	10m	10km
	Wireless	135m	500m	40cm	400m	-	10km	1.5m	-	-	100m
MDM		-	LG	LG	LG	OAM	-	-	-	-	HG
Transmission		Unidirectional	Unidirectional	Unidirectional	Unidirectional	Unidirectional	Unidirectional	Unidirectional	Unidirectional	Unidirectional	Bidirectional
Weather conditions		-	Clear air, haze, rain fog, dust	-	Light and heavy dust	-	-	-	Light haze, medium and dense fog	-	Clear air, haze, rain, fog
Atmospheric turbulence		Non-uniform turbulence	-	-	Strong	-	Moderate-strong	-	-	-	Weak
Geometric loss		-	Yes	-		-	-	-	-	-	Yes
Beam divergence		-	Yes	-	0.2mrad	-	-	-	-	-	10
Additional loss		-	-	-	-	-	-	-	-	-	5dB
Complexity		Complex	Low	Medium	Complex	Complex	Complex	Low	Medium	Medium	Low
Cost		High	Low	Moderate	High	High	High	Low	Moderate	Moderate	Low

Table 6 illustrates that the proposed RoF-MDM system allows a bidirectional signal transmission over SMF-FSO link. Although, achieved data rate (=1Gbps) is lowest in the proposed system but it also faces less channel interference in bidirectional due to lowest launched power (=6dBm) compared to prior works. Also, maximum wired-wireless range in Refs. [9] and [10] is larger than the proposed system but the impact of additional loss is not considered as in this work. In short, under the impact of highest link distortions and atmospheric conditions, the proposed work is a good example of a future based optical-RF based system incorporating MDM beams over integrated fiber-FSO link. Besides this, the major issues like mode crosstalk, high attenuation, misalignment, system complexity as well as power constraints can be seen that can lead to limited communication range, lower throughput, higher error rate and prone to link losses. For this, machine-learning basics MDM-RoF system can be realized. These findings have realistic implications for FSO systems, highlighting the significance of advanced synchronization to solve phase errors. The trade-offs between transmission distance and data rate, robustness, and complexity must be carefully investigated during the system design.

4. Conclusion

A full-duplex and symmetric 1Gbps MDM-RoF system using integrated SMF-FSO link is realized. Four HG modes i.e. HG[0,0], HG[1,0], HG[2,0] and HG[3,0] modes are used to evaluate the system performance under different weather conditions. It is concluded that maximum FSO range of 100m in downlink and 14-17m in uplink transmission is achieved, under clear air, haze, rain and fog conditions, with fixed 10km SMF. Also, the system using integrated 10km SMF with 10m FSO distance under clear air scenario, can sustain maximum beam divergence of 10mrad in downlink and 3.5mrad in uplink directions. Moreover, at BER limit of 10^{-9} maximum additional losses of 2.5-5dB and 0-0.3dB in downlink and uplink respectively, can be sustained. As compared to previous designs, this work offers less power loss over integrated wired-wireless distant with high capacity, low cost and simple full-duplex architecture under severe atmospheric conditions. In future this design can be utilized for integrated fiber-wireless based system in rural to urban areas with high channel capacity. Moreover, it can be used for high-capacity mobile fronthaul/backhaul, data center interconnects, outdoor/indoor wireless coverage, mmW wireless access, THz communications, Internet of Things (IoT), smart cities, military and satellite ground station scenarios.

References

[1] J. Ma, M. Zhou, Y. Zhan, H. Liang, C. Yu, Opt. Laser Technol. **46**, 81 (2013).
[2] B. J. Hamza, W. K. Saad, I. Shayea, N. Ahmad, N. Mohamed, D. Nandi, G. Golshan, IEEE Access **9**, 49487 (2021).
[3] H. Khalil, F. Qamar, R. Shahzadi, A. Shahzad, M. Ali, N. Qamar, S. Al-Otaibi, IEEE Access **9**, 139393 (2021).
[4] Q. Ding, M. Wang, H. Mu, Y. Tang, J. Zhang, B. Wu, T. Li, Opt. Commun. **427**, 54 (2018).
[5] Y. Shao, Opt. Laser Technol. **77**, 59 (2016).
[6] A. M. Ragheb, Q. Tareq, M. A. Esmail, H. Fathallah, S. A. Alshebeili, M. Z. M. Khan, IEEE J. Sel. Top. Quantum Electron. **29**, 1 (2023).
[7] Y. Wu, J. Wen, M. Zhang, J. Wen, W. Chen, X. Zhang, F. Pang, F. Tang, G. West, T. Wang, J. Light. Technol. **40**, 7922 (2022).
[8] G. S. D. Gordon, M. J. Crisp, R. V. Penty, T. D. Wilkinson, I. H. White, Journal of Lightwave Technology **32**, 3521 (2014).
[9] A. Sood, R. Kaushik, J. Opt. **53**, 1095 (2024).
[10] D. N. Nguyen, L. Vallejo, J. Bohata, B. Ortega, Z. Ghassemlooy, S. Zvanovec, Opt. Commun. **475**, 126281 (2020).
[11] A. Minoofar, X. Su, H. Zhou, R. Zhang, F. Alishahi, K. Zou, H. Song, K. Pang, S. Zach, M. Tur, A. F. Molisch, H. Sasaki, D. Lee, A. E. Willner, Journal of Lightwave Technolology **40**, 3285 (2022).
[12] S. Sinha, C. Kumar, Opt. Appl. **LIII**, 431 (2023).
[13] Z. Guo, B. Liu, J. Ren, Y. Li, Y. Mao, X. Wu, R. Ullah, B. Wang, F. Wang, L. Zhao, Y. Li, S. Zhou, M. Wu, Journal of Lightwave Technology **42**, 1886 (2024).
[14] B. Schrenk, J. Light. Technol. **43**, 1067 (2025).
[15] M. Zhu, L. Zhang, S. H. Fan, C. Su, G. Gu, G. K. Chang, IEEE Photonics Technol. Lett. **24**, 1127 (2012).
[16] R. Kaur, R. S. Kaler, J. Electr. Eng. **72**, 46 (2021).
[17] V. Arya, J. Opt. Commun. **0**, 1 (2025).
[18] A. Niaz, F. Qamar, M. Ali, R. Farhan, M. K. Islam, Trans. Emerg. Telecommun. Technol. **30**, 1 (2019).
[19] M. S. Awan, L. Csurgai-Horváth, S. S. Muhammad, E. Leitgeb, F. Nadeem, M. S. Khan, J. Commun. **4**, 533 (2009).
[20] K. Zou, K. Pang, H. Song, J. Fan, Z. Zhao, H. Song, R. Zhang, Nat. Commun. **13**, 7662 (2022).
[21] Y. Wen, F. Yang, J. Song, Z. Han, IEEE Internet Things J. **12**, 2158 (2023).
[22] O. Balasiano, E. Wohlgemuth, I. Attia, A. Roizman, T. Falk, R. Vered, and D. Sadot, J. Light. Technol. **42**, 7085 (2024).
[23] T. Umezawa, A. Matsumoto, A. Kanno, K. Akahane, N. Yamamoto, Journal of Lightwave Technolology **42**, 1328 (2024).
[24] B. Mallick, P. Parida, C. Nayak, T. Khalifa, M. K. Panda, N. Ali, G. U. Patil, B. Prasad, IEEE Access **13**, 62476 (2025).

*Corresponding author: meetkumari08@yahoo.in